

# Multi-objective optimization of process parameter in Activated Tungsten Inert Gas (A-TIG) Welding

S. I. Bachani and N. D. Ghetiya

**Abstract**— Tungsten Inert Gas (TIG) welding is a process which is used in those applications requiring a high degree of quality and accuracy. However, this welding process has the disadvantage of less productivity. To overcome this disadvantage, Activated Tungsten Inert Gas (A-TIG) welding was developed. In the present work, experiments were performed on 6 mm thick 304L stainless steel plates using A-TIG welding process. TIG welding fixture was designed and developed for getting fixed arc length and different welding speeds. Three different combinations of fluxes like  $TiO_2 + MnO_2$ ,  $SiO_2 + TiO_2$ , and  $Al_2O_3 + CaO$  were used to investigate its effect on geometric shape and distortion of weldment. A-TIG welding process parameters optimization was performed by a multi-objective optimization technique named as Grey Principal Component Analysis (G-PCA). The optimum process parameters were found to be 140 A current, 100 mm/min speed and a mixture of  $SiO_2$  and  $TiO_2$  flux.

**Index Terms**— Activated Tungsten Inert Gas welding, welding fixture, Grey Principal Component Analysis, Multi-objective optimization

## Nomenclature

$\epsilon_i$	Grey Relational Coefficient
$\xi$	Distinguishing Coefficient
$\Delta$	Deviation Sequence
$\gamma_i$	Grey Relational Grade
$R_{ji}$	Coefficient Array
$\lambda_k$	Eigen Value

## I. INTRODUCTION

TUNGSTEN Inert Gas (TIG) welding is a process which is used in those applications requiring a high degree of quality and accuracy. However, this welding process has low penetration depth and productivity due to a combination of low deposited rate and shallow joint penetration. A-TIG welding process is used to increase the penetration during welding of stainless steel. Many researchers focused their investigation on the A-TIG welding of steel. Austenitic stainless steels, particularly AISI 304L, widely used in engineering applications, such as in the manufacturing, chemical, nuclear, food industries as well as oil and petrochemical [1,2]. Research papers are available in the area of application of A-TIG for various

ferrous, nonferrous and dissimilar materials [3, 4]. A-TIG welding was carried out on dissimilar plates with 6 mm thickness and the results were indicated that it could increase the welding depth as well as decreased the weld width than TIG welding process [5, 6]. In the A-TIG welding, fluxes mixed with carrier solvents like acetone, methanol, and ethanol and applied on the surface base material to be welded. Fluxes were melted and vaporized during experiments. As a result penetration depth was increased, weld width was decreased and mechanical properties were improved [7, 8, 9]. Some researchers [10, 11] observed that greater penetration was achieved by constriction of an electric arc in A-TIG welding. Arc constriction can increase the anode current density and the arc force acting on the weldment. Marangoni convection is responsible for the increase in weld penetration depth due to change in the liquid flow of molten metal in weldment. It is caused by oxygen content in activated flux [12, 13]. An objective of the work is to investigate the influence of different kinds of combination of oxide fluxes such as  $TiO_2 + MnO_2$ ,  $SiO_2 + TiO_2$ , and  $Al_2O_3 + CaO$  on the weld geometric shape and deformation. A-TIG welding parameters are optimized by a multi-objective optimization technique known as Grey Principal Components Analysis (G-PCA).

## II. EXPERIMENTATION

Welding was carried out on 6 mm thick stainless steel 304L plates whose chemical composition and mechanical properties are shown in Table 1 and Table 2. SS 304L plates were cut into  $150 \times 75$  mm strips for A-TIG welding. Activated flux was prepared using three kinds of combination oxides ( $TiO_2 + MnO_2$ ,  $SiO_2 + TiO_2$  and  $Al_2O_3 + CaO$ ) packed in powdered form. These powders were mixed with methanol to produce paint like consistency. A thin layer of the flux was applied before welding on the surface of a base metal to be welded. A-TIG experiment was carried out as per the Taguchi design. Welding fixture was designed and developed for getting fixed arc length and different welding speed, as shown in Fig. 1.

S. I. Bachani, Mechanical Engineering Department, Dr. Jivraj Mehta Institute of Technology, Anand, Gujarat  
(E-mail: bachanisunil10@gmail.com).

N. D. Ghetiya, Mechanical Engineering Department, Institute of Technology, Nirma University, Ahmedabad, Gujarat  
(E-mail: Nilesh.ghetiya@nirmauni.ac.in)

TABLE 1.  
CHEMICAL COMPOSITION OF STAINLESS STEEL 304L

C	Si	Mn	P	Cr	Ni	S	N	Fe
0.03	0.75	2.0	0.045	18.0	10.0	0.03	0.1	Bal.

TABLE 2.  
PROPERTIES OF STAINLESS STEEL 304L

Tensile Strength MPa	Density Kg/m <sup>3</sup>	Thermal conductivity W/m-k	Melting point °C	Hardness HRB
586	8030	16.2	1399	82

Welding parameters used for fabrication of joints are shown in Table 3. After welding, angular distortion was measured and method for the same is shown in Fig. 2. The angular distortion  $\theta$  can be derived from equation (1).

$$\theta = \tan^{-1} \frac{AC}{30} + \tan^{-1} \frac{BD}{30} \tag{1}$$



Fig. 1. A-TIG welding set up

TABLE 3  
WELDING PARAMETERS

Parameters	Values
Welding current	60- 140 A
Welding speed	80-160 mm/min
Activated Flux	TiO <sub>2</sub> + MnO <sub>2</sub> , SiO <sub>2</sub> + TiO <sub>2</sub> , Al <sub>2</sub> O <sub>3</sub> + CaO
Gas flow rate	10 L/min
Electrode diameter	4 mm
Tip angle	75 degree
Arc length	2 mm
Shielding gas	Argon

The specimens were cut from the strip with the use of a power hacksaw machine for the weld bead observation and microstructure examination. All these specimens were prepared by grinding, polishing and then followed by etching in a solution of 10 g CuSO<sub>4</sub> + 50 ml HCL and swab with soft cotton for few seconds. Tool maker’s microscope was used to measure weld bead width and depth. The microstructure of different zones like weld metal, base metal and fusion boundary under different flux combination were viewed and captured by using an inverted optical microscope coupled with image analyzer software.

III. ANALYSIS METHOD

A. Grey Relational Analysis (GRA)

1) Data Processing

GRA is measures the correlation degree among factors based on the similarity or difference among it. It involves data processing and calculation according to the quality characteristics. Calculate method of the grey relational generation is as follows:

The larger the better characteristic (higher the target value, the better)

$$Z_{ij} = \frac{Y_{ij} - \min(Y_{ij,i=1,2,\dots,n})}{\max(Y_{ij,i=1,2,\dots,n}) - \min(Y_{ij,i=1,2,\dots,n})} \tag{2}$$

The smaller the better characteristic (smaller the target value, the better)

$$Z_{ij} = \frac{\max(Y_{ij,i=1,2,\dots,n}) - Y_{ij}}{\max(Y_{ij,i=1,2,\dots,n}) - \min(Y_{ij,i=1,2,\dots,n})} \tag{3}$$

Nominal the better characteristic (if target specify value, set tatget value OB)

$$Z_{ij} = 1 - \frac{|Y_{ij} - OB|}{\max\{\max Y_{ij} - OB, OB - \min Y_{ij}\}} \tag{4}$$

Where Z<sub>ij</sub> is the sequence after data processing; Y<sub>ij</sub> is original sequence of responses. Max Y<sub>ij</sub> is maximum value of Y<sub>ij</sub> and min Y<sub>ij</sub> is minimum value of Y<sub>ij</sub>.

2) Grey Relational Coefficient and Grey Relational Grade

It is expressed the relationship between the best and the actual experimental results from sequence after data processing using equation (5).

$$\epsilon_i [Y_0, Y_i] = \frac{\Delta \min + \xi \Delta \max}{\Delta \min + \xi \Delta \max} \tag{5}$$

Where i= 1, 2...n: n is the number of the trials. Δ0i is deviation sequence of the reference Sequence. i.e Δ0i = |Y0 - Yi| is the absolute value of difference between Y0 and Yi.

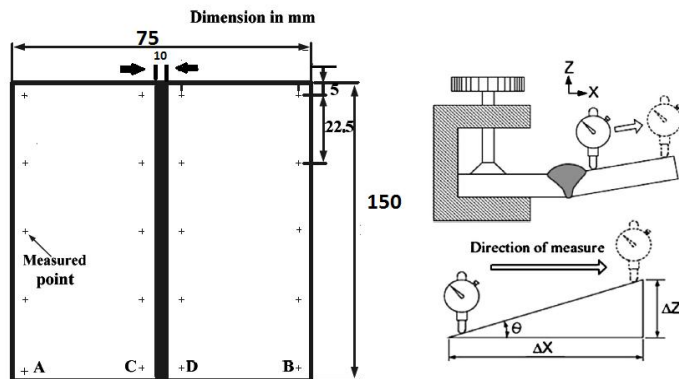


Fig. 2. Schematic diagram of weld distortion measurement [14].

$\Delta_{\min}$  is minimum value of  $\Delta 0_i$  and  $\Delta_{\max}$  is maximum value of  $\Delta 0_i$ .

$\xi$  is the distinguishing coefficient whose value is taken to be 0.5 due to equal importance for all the responses.

The average of the grey relational coefficient is then calculated to obtain grey relational grade. The grey relational grade is defined as follows:

$$\gamma_i = \frac{1}{n} \sum_{k=1}^n \varepsilon_i \tag{6}$$

However the effect of each factor on the system is not exactly the same in real application. Thus equation (6) can be modified as follows:

$$\gamma_i = \sum_{k=1}^n c_k \cdot \varepsilon_i \tag{7}$$

Where  $C_k$  represents the weighting value of factor  $k$ .

In GRA, the grey relational grade is used to show the relationship between quality characteristics. If two sequences are identical, the value of the grey relational grade is equal to one. Grey analysis is actually a measurement of an absolute value of data difference between sequences and it could be used to measure approximation correlation sequences.

**B. Principal Component Analysis**

Principal Component Analysis (PCA) explains the structure of variance covariance by the linear combinations of each quality characteristic.

The original multiple quality characteristic array

$$Y_i(j), i=1, 2, \dots, m; j=1, 2, \dots, n \tag{8}$$

$$A = \begin{bmatrix} Y_1(1) & Y_1(2) & \dots & Y_1(n) \\ \vdots & \vdots & \dots & \vdots \\ Y_m(1) & Y_m(2) & \dots & Y_m(n) \end{bmatrix}$$

Where  $m$  is the number of trials and  $n$  is the number of the quality characteristic. In this paper  $Y$  is the grey relational coefficient of each quality characteristic and  $m = 18, n = 3$ .

Co-relation Coefficient Array is calculated as following equation:

$$R_{ji} = \left( \frac{Cov(Y_i(j), Y_i(l))}{\sigma_{Y_i(j)} \times \sigma_{Y_i(l)}} \right); j=1, 2, \dots, n; l=1, 2, \dots, n \tag{9}$$

where  $Cov(Y_i(j), Y_i(l))$  are covariance sequence  $Y_i(j)$  and  $Y_i(l)$  respectively  $\sigma_{Y_i(j)}$  is the standard deviation of sequence  $Y_i(j)$ ,  $\sigma_{Y_i(l)}$  is the standard deviation of sequence  $Y_i(l)$ .

Calculate the Eigen values and Eigen vectors are determine from the correlation coefficient array

$$(R - \lambda_k I_m) S_{ik} = 0 \tag{10}$$

Where  $\lambda_k$  is an Eigen value,  $\sum_{k=1}^n \lambda_k = n$  and  $k = 1, 2, \dots, n$ ;  $S_{ik} = [ak1, ak2, \dots, akn]$  correspond to Eigen value  $\lambda_k$

The principal component is formulated as follows;

$$P_{mk} = \sum_{i=1}^n Y_m(i) \cdot S_{ik} \tag{11}$$

Where  $P_{m1}$  is the first principal component,  $P_{m2}$  is the second principal component and so on.

**IV. EXPERIMENTAL DESIGN AND RESULTS**

**A. Experimental Design**

A-TIG welding process was correlated with process parameters such as welding speed, welding current, activated flux, that were regards as controllable factors in this study. They were varied at three level and an orthogonal L18 array was used to conduct the experiments for various combination of inputs and responses as indicated in Table 4 and Table 5.

TABLE 4. PROCESS PARAMETERS AND THEIR LEVELS

Process parameter	Unit	Level		
		1	2	3
Current	A	60	100	140
Welding Speed	mm/min	100	125	150
Flux	-	TiO <sub>2</sub> + MnO <sub>2</sub>	SiO <sub>2</sub> + TiO <sub>2</sub>	Al <sub>2</sub> O <sub>3</sub> + CaO

TABLE 5. EXPERIMENTAL DESIGN (L18) AND RESPONSES

Trial	Input Parameters			Responses		
	Current	Speed	Flux	Penetration (mm)	Width (mm)	Distortion (Degree)
1	60	100	1	0.99	4.5	1.22
2	60	125	2	1.37	3.1	1.34
3	60	150	3	1.27	4.25	2.76
4	100	100	1	1.16	5.65	2.77
5	100	125	2	1.4	3.9	2.97
6	100	150	3	2.47	4.04	3.05
7	140	100	2	3.64	3.75	0.76
8	140	125	3	3.38	3.95	1.57
9	140	150	1	2.62	6.95	1.79
10	60	100	3	2.34	2.51	1.26
11	60	125	1	0.5	3.53	2.26
12	60	150	2	1.43	4.02	2.58
13	100	100	2	1.07	3.6	1.95
14	100	125	3	2.4	3.7	2.03
15	100	150	1	1.29	5.99	3.77
16	140	100	3	3.4	3.58	1.5
17	140	125	1	2.91	3.95	1.87
18	140	150	2	4.06	4.28	1.75

**B. Analysis Method**

The algorithm grey relational analysis coupled with the principal component analysis is used to determine a combination of the process parameters for the A-TIG welding process.

*Step 1- Calculate the sequence after data processing:*

In GRA, the experimental results for sequence after data processing of responses in penetration depth, weld width, and distortion in Table 5 are evaluated according to larger the better characteristics and smaller the better characteristics of the sequence by using equation (2)

(3). All the sequence after data processing can be calculated as follows and values are listed in Table 6. A larger value of results corresponds the better performance and the maximum results that are equal to lindicated best performance.

$$Z01(1) = \frac{0.99 - 0.5}{4.06 - 0.5} = 0.138$$

$$Z01(2) = \frac{6.95 - 2.51}{6.95 - 4.5} = 0.551$$

$$Z01(3) = \frac{3.769 - 1.215}{3.769 - 0.76} = 0.849$$

According to Table 6, the deviation sequences Δ01 can be calculated as follows:

$$\Delta 01(1) = |1.000 - 0.138| = 0.862$$

$$\Delta 01(2) = |1.000 - 0.551| = 0.449$$

$$\Delta 01(3) = |1.000 - 0.849| = 0.151$$

Therefore Δ01 = (0.862, 0.449, 0.151) the same calculating method is performed for i=1, 2, 3...18 and values are listed in Table 7. By the investigating the data presented in Table 7, Δmax and Δmin can be expressed as follows:

$$\Delta_{max} = \Delta_{11}(1) = \Delta_{09}(2) = \Delta_{15}(3) = 1.000$$

$$\Delta_{min} = \Delta_{18}(1) = \Delta_{10}(2) = \Delta_{07}(3) = 0.000$$

TABLE 6.  
SEQUENCE AFTER DATA PROCESSING

Trial	Penetration	Width	Distortion
Reference Sequence	1.000	1.000	1.000
1	0.138	0.551	0.849
2	0.244	0.867	0.807
3	0.216	0.608	0.334
4	0.185	0.293	0.332
5	0.253	0.687	0.265
6	0.553	0.655	0.241
7	0.882	0.720	1.000
8	0.809	0.676	0.731
9	0.600	0.000	0.658
10	0.517	1.000	0.834
11	0.000	0.770	0.501
12	0.261	0.660	0.396
13	0.160	0.755	0.605
14	0.531	0.732	0.577
15	0.222	0.216	0.000
16	0.815	0.760	0.754
17	0.677	0.676	0.632
18	1.000	0.601	0.671

Step 2- Calculate of the Grey Relational Coefficient of Response variables:

The grey relational coefficient for the each quality characteristic were calculated by substituting the distinguishing coefficient ξ = 0.5 by using equation (5). Grey relational coefficients Ε i were calculated as follows:

$$\epsilon 1(1) = \frac{0.000 + (0.5)(1.000)}{0.862 + (0.5)(1.000)} = 0.367$$

$$\epsilon 1(2) = \frac{0.449 + (0.5)(1.000)}{0.449 + (0.5)(1.000)} = 0.448$$

$$\epsilon 1(3) = \frac{0.151 + (0.5)(1.000)}{0.151 + (0.5)(1.000)} = 0.768$$

TABLE 7.  
DEVIATION SEQUENCE

Trial	Penetration	Width	Distortion
1	0.862	0.448	0.151
2	0.756	0.133	0.193
3	0.784	0.392	0.666
4	0.815	0.707	0.668
5	0.747	0.313	0.735
6	0.447	0.345	0.759
7	0.118	0.280	0.000
8	0.191	0.324	0.269
9	0.404	1.000	0.342
10	0.483	0.000	0.166
11	1.000	0.230	0.499
12	0.739	0.340	0.604
13	0.840	0.245	0.395
14	0.466	0.268	0.423
15	0.778	0.784	1.000
16	0.185	0.271	0.246
17	0.323	0.324	0.368
18	0.000	0.400	0.329

Thus Ε 1 (k) = (0.367, 0.448, 0.768), k = 1, 2, 3. Similar procedure was applied for i = 1, 2...18. Table 8 lists the grey relational coefficient for each trial of the L18 OA.

TABLE 8.  
GREY RELATIONAL COEFFICIENTS

Trial	Penetration	Width	Distortion
1	0.367	0.527	0.768
2	0.398	0.790	0.722
3	0.389	0.561	0.429
4	0.380	0.414	0.428
5	0.400	0.615	0.405
6	0.528	0.592	0.397
7	0.809	0.642	1.000
8	0.724	0.607	0.650
9	0.553	0.333	0.594
10	0.509	1.000	0.751
11	0.333	0.985	0.500
12	0.404	0.595	0.453

13	0.373	0.971	0.558
14	0.517	0.651	0.541
15	0.391	0.389	0.333
16	0.730	0.675	0.670
17	0.608	0.607	0.576
18	1.000	0.559	0.603

Step 3 – Computation of the contribution of respective quality characteristics by using Principal Component Analysis (PCA):

In order to objectively reflect the relative importance for each quality characteristic in GRA, PCA was used to determine the corresponding weighting values for each quality characteristic. Grey relational coefficient of each quality characteristic is listed in Table 8. These data were used to assess the correlation coefficient matrix and determine the eigenvalues from equation (10) shown in Table 9. The eigenvector corresponding to each eigenvalue is listed in Table 10 and its square represents the contribution of the corresponding quality characteristic to the principal component.

TABLE 9.

EIGEN VALUES AND EXPLAINED FOR PRINCIPAL COMPONENT

Principal component	Eigen value	Explained variation (%)
First	1.643	54.775
Second	0.970	32.340
Third	0.385	12.885

TABLE 10.

EIGEN VECTOR FOR PRINCIPAL COMPONENT

Quality characteristic	First	Second	Third
Penetration Depth	0.528	-0.672	-0.520
Width	0.483	0.741	-0.467
Distortion	0.699	-0.005	0.715

TABLE 11.

CONTRIBUTION OF QUALITY CHARACTERISTIC FOR THE PRINCIPAL COMPONENT

Quality characteristic	Contribution
Penetration Depth	0.461
width	0.203
Distortion	0.336

The contribution of responses in the penetration depth, weld width and distortion of the A-TIG weldment is shown in Table 11. These contribution were listed as 0.461, 0.203 and 0.336 respectively. Moreover the variance contribution for the first principal component characteristic the three quality characteristic was as high 54.775%. Therefore, for this study the squares of the respective eigenvectors were selected as the weighting values of the related quality characteristic. Coefficients C<sub>1</sub>, C<sub>2</sub>, and C<sub>3</sub> in equation (7) were set as 0.461, 0.203, and 0.336 respectively.

Using equation (7) and the data listed in Table 8 the grey relational grades were evaluated as follows:

$$\gamma_1 = (0.461 \times 0.367) + (0.203 \times 0.527) + (0.336 \times 0.768) = 0.534$$

By using the same procedure, the grey relational grade of the comparability sequence for i = 1-18 can be obtained and is presented in Table 12. The processing parameters were optimized with respect to single grey relational grade rather than complicated multiple quality characteristics.

TABLE 12.

GREY RELATIONAL AND ITS ORDER

Trial	Grade	Order
1	0.534	9
2	0.586	7
3	0.437	16
4	0.403	17
5	0.446	15
6	0.497	11
7	0.839	1
8	0.675	5
9	0.522	10
10	0.690	4
11	0.461	13
12	0.459	14
13	0.496	12
14	0.552	8
15	0.371	18
16	0.699	3
17	0.597	6
18	0.777	2

Step 4 – Optimal combination of process parameters:

To determine the optimal combination of process parameters for responses in penetration depth, weld width and distortion of the A-TIG welding. The average grey relational grade for each process parameters level was evaluated by employing the main effect analysis of the Taguchi method. This process was performed by sorting the grey relational grades corresponding to the levels of the process parameters in each column of the OA and then taking the average of parameters with the same levels. i.e for factor A (Table 5) experiments 1, 2, and 3 were set to level 1. Therefore by using the data listed in Table 12, the average grey relational grade for A1 was evaluated as follows:

$$A_1 = \frac{0.534+0.612+0.447+0.720+0.482+0.470}{6} = 0.544$$

$$A_2 = \frac{0.406+0.458+0.499+0.514+0.560+0.371}{6} = 0.468$$

$$A_3 = \frac{0.832+0.668+0.510+0.695+0.596+0.747}{6} = 0.675$$

By using a similar method, evaluations were performed for each process parameter level and the main effect analysis was developed which is shown in Fig. 3. Considering that the grey relational grade was represented by the level of correlation between the reference and comparability sequence. A larger grey relational grade was indicated that the comparability sequence exhibited stronger correlation with the reference sequence. Fig. 3 shows that the multiple quality characteristics of the A-TIG welding were significantly affected by changing the processing parameters. From the response table for the grey relational grade shown in Table 13, the best combination of process parameters was A<sub>3</sub> (current of 140 A), V<sub>1</sub> (welding speed of 100 mm/min), and F<sub>2</sub> (mixture of flux TiO<sub>2</sub> and SiO<sub>2</sub>).

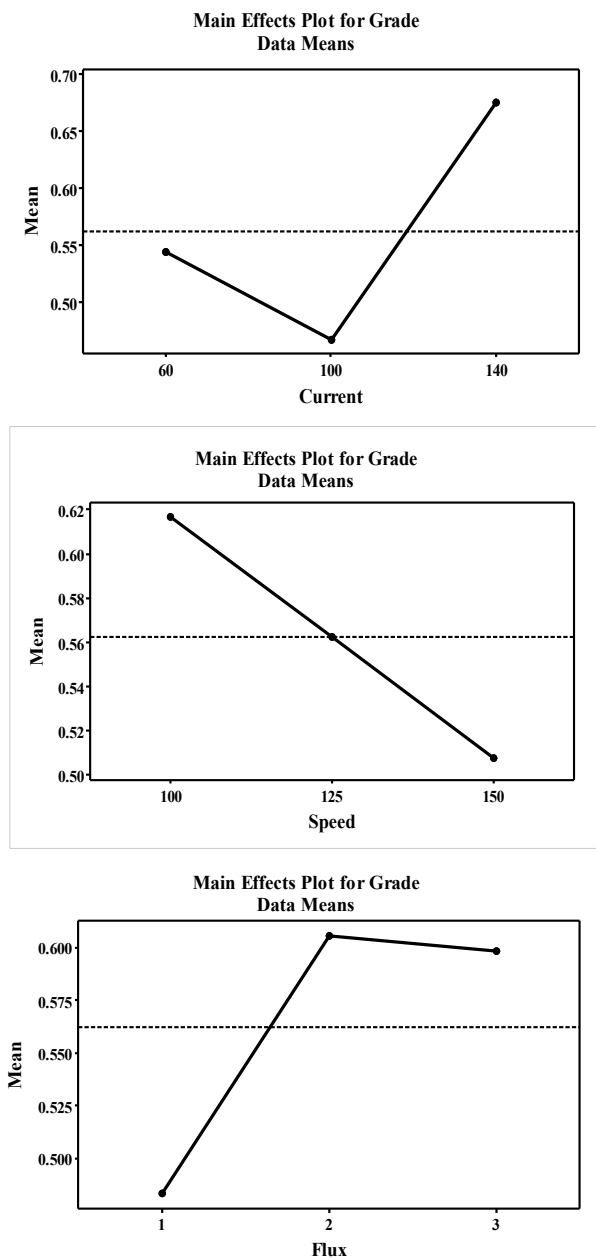


Fig. 3. Effect of process parameter levels on multiple quality characteristics

TABLE 13.  
RESPONSE TABLE FOR GREY RELATIONAL GRADE

Symbol	Process Parameter	Level 1	Level 2	Level 3
A	Current	0.544	0.468	0.675
V	Speed	0.617	0.563	0.508
F	Flux	0.483	0.606	0.598

*Step 5- Analysis of Variance (ANOVA):*

ANOVA analysis was carried out using Minitab software. ANOVA results for the grey relational grades are listed in Table 14. It shows that the two parameters current and flux are found to be the major factors with the selected multiple quality characteristics. The significance of each process parameter in the responses in penetration depth, weld width and distortion of the A-TIG welding process can be determined by the percentage contribution.

TABLE 14  
RESULT OF ANOVA

Symbol	Process Parameter	DOF	SS	MS	F-value	Contribution (%)
A	Current	2	0.1311	0.0656	14.23	47.81
V	Speed	2	0.0359	0.0179	3.89	13.09
F	Flux	2	0.0565	0.0283	6.13	20.61
Error		11	0.0507	0.0046		18.49
Total		17	0.2742			

R Squared – 81.51%

From the results of ANOVA, current appears to be most important processing parameter with the highest percentage contribution of 47.81% which increases penetration depth and reduced weld width as well as distortion of the A-TIG welding.

*C. Geometric shape of A-TIG welds*

Oxygen is the surface active trace element most commonly found in steel alloy. When TIG welding used with oxide flux powder, a temperature coefficient of surface tension shows negative to positive value. Due to this active trace element surface tension achieved higher value at the center region of the weld pool. A result of the positive value of surface tension gradient reverse Marangoni convection is existed in weld pool [13]. The effect can be observed from the weld shape. Fig.4 shows the transverse cross-sections of A-TIG welds with different oxide flux. Fig. 4(a) and Fig. 4(c) shows that A-TIG weld is made with SiO<sub>2</sub> + TiO<sub>2</sub> produced deep and narrow weld shape. These results show that using SiO<sub>2</sub> and TiO<sub>2</sub> fluxes created a significant increase in penetration depth and a decrease in weld width Fig. 4(d) and Fig. 4(f) show that wide and shallow weld shape produced by using TiO<sub>2</sub> + MnO<sub>2</sub>. These results show that MnO<sub>2</sub> flux has a negative effect on the A-TIG weld morphology. It is clear that different weld penetration and width obtained with the use of different oxide compound during A-TIG welding







Macrostructure	Input Parameters	Responses
 <p>(a)</p>	Current-140A Speed-150 mm/min Flux- SiO <sub>2</sub> + TiO <sub>2</sub>	Penetration- 4.06mm Width- 4.28mm
 <p>(b)</p>	Current-100A, Speed-125 mm/min Flux- Al <sub>2</sub> O <sub>3</sub> + CaO	Penetration- 2.4mm Width- 3.7mm
 <p>(c)</p>	Current-140A Speed-100 mm/min Flux- SiO <sub>2</sub> + TiO <sub>2</sub>	Penetration- 3.38mm Width- 3.95mm
 <p>(d)</p>	Current-60A Speed-150 mm/min Flux- TiO <sub>2</sub> + MnO <sub>2</sub>	Penetration- 1.37mm Width- 3.1mm
 <p>(e)</p>	Current-100A Speed-125 mm/min Flux- SiO <sub>2</sub> + TiO <sub>2</sub>	Penetration- 1.4mm Width- 3.9mm
 <p>(f)</p>	Current-100A Speed-100 mm/min Flux- TiO <sub>2</sub> + MnO <sub>2</sub>	Penetration- 1.16mm Width- 5.65mm

Fig. 4. Effect of oxide compound on geometric shape of A-TIG welds

*D. Angular Distortion of A-TIG welds*

Deformation is occurred due to solidification shrinkage and thermal contraction in weld pool and base metal during quickly heating and cooling cycle. Fig.5 shows the angular distortion of A-TIG welding made with a different combination of oxide compound. The angular distortion of the weldment made with a mixture of SiO<sub>2</sub> and TiO<sub>2</sub> is reduced compared with the other two combinations. The angular distortion of weldment depends on the ratio of the weld depth and plate thickness and it also depends on the power density of the welding heat source. It is increased with increasing weld current.

Angular distortion of weldment is decreased at shallow depth and increased with increasing ratio of penetration depth and plate thickness in A-TIG welding process to the critical point at 100 A. When penetration depth exceed half of the plate thickness the angular distortion is decreased at a current greater than 100 A. Penetration depth is increased and angular distortion is decreased in A-TIG welding which indicates that arc is generated with higher energy density. As the arc energy density is increased the overall heat energy required per unit length of weld deposit is decreased. This factor to a reduction in the quantity of supplied heat thereby it prevents the base material from overheating and

reduced the occurrence of thermal stress and contrary strain caused by shrinkage in thickness [5]. Consequently, A-TIG welding can reduce the angular distortion of the weldment.

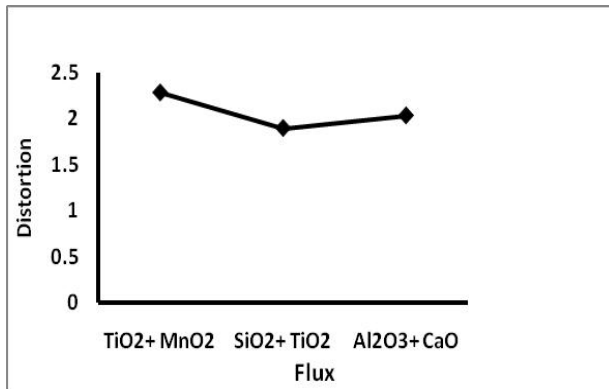


Fig. 5. Angular distortion of A-TIG weldment

## V. CONCLUSIONS

Following conclusions are drawn from the present work:

- The maximum penetration, minimum weld width, and angular distortion are achieved in A-TIG welding with a mixture of SiO<sub>2</sub> and TiO<sub>2</sub> fluxes. Also, minimum penetration and maximum weld width, as well as angular distortion, is noticed while using a mixture of TiO<sub>2</sub> and MnO<sub>2</sub>.
- The maximum penetration of 3.64 mm, minimum weld width of 3.76 mm, as well as angular distortion of 0.76°, is obtained at optimized parameters of current 140 A, welding speed 100 mm/min and mixture of SiO<sub>2</sub> and TiO<sub>2</sub> flux respectively in A-TIG welding process.
- The A-TIG welding increases the arc voltage and the amount of heat input per unit length in the weld and therefore the delta ferrite content in weldment is increased.

## REFERENCES

- [1] Davis, J.R.; *Stainless steel*. In ASM Specialty Handbook, 1st ed.; ASM International: Northeast, OH, USA, 1994.
- [2] Beddoes, J.; Parr, J.G. *Introduction to Stainless Steels*, 3rd ed.; ASM International: Northeast, OH, 1999.
- [3] Modensi PJ, Apolingaro ER, Pereira IM (1998) TIG welding with single component flux. *Journal of Material Processing Technology*, July, 260–265.
- [4] Huang HY, Shyu SW, Tseng KH, Chou CP. (2005) Evaluation of TIG flux welding on the characteristics of stainless steel. *Science and Technology of Welding and Joining*; 10, 566–573.
- [5] Cheng-Hsien Kuo, Kuang-Hung Tseng and Chang-Pin Chou. (2011) Effect of activated TIG flux on performance of dissimilar welds between mild steel and stainless steel, *Key Engineering Materials* 479, 74-80.
- [6] A. Berthier, P. Paillard, M. Carin, F. Valensi and S. Pellerin. 'TIG and A-TIG welding experimental investigations and comparison to simulation Part 1: Identification of Marangoni effect', *Science and technology of welding and joining* 2012 17 (8), 609-615.
- [7] Paulo J. Modenesi, Eustaquio R. Apolinario and Iaci M. Pereira. (2000) TIG welding with single component fluxes, *Journal of Materials Processing Technology* 99, 260-265.
- [8] B. Arivazhagan and M. Vasudevan. (2014) A comparative study on the effect of GTAW processes on the microstructure and mechanical properties of P91 steel weld joints', *Journal of Manufacturing Processes* 16, 305–311.
- [9] G. Ruckert, B. Huneau and S. Marya. (2007) Optimizing the design of silica coating for productivity gains during the TIG welding of 304L stainless steel', *Material and Design* 28, 2387-2393.
- [10] Li Qing-ming, Wang Xin-hing, Zou Zeng-da, Wu Jun. (2007) Effect of activating flux on arc shape and arc voltage in tungsten inert gas welding. *Transactions of Non-ferrous Metal Society of China*, February, 486–490.
- [11] Kuo Cheng-Hsien, Tseng Kuang-Hung, Chou Chang-Pin. (2011) Effect of activated TIG flux on performance of dissimilar welds between mild steel and stainless steel. *Key Engineering Materials*; 479, 74–80.
- [12] Huang HY, Shyu SW, Tseng KH, Chou CP. (2007) Study of the performance of stainless steel A-TIG welds. *Journal of Material Engineering and Performance*, March 17(2), 193–201.
- [13] Shaping Lu, Hidetoshi Fujii, Hiroyuki Sugiyama, Manabu Tanaka and Kiyoshi Nogi. (2002) Weld Penetration and Marangoni convection with Oxide Fluxes in GTA Welding', *Material Transactions* 43 (11), 2926-2931.
- [14] Sanjay G. Nayee and Vishvesh J. Badheka. (2014) Effect of oxide based fluxes on mechanical and metallurgical properties of Dissimilar Activating Flux Assisted-Tungsten Inert Gas Welds', *Journal of Manufacturing Processes* 16, 137–143.
- [15] Huang HY, Shyu SW, Tseng KH, Chou CP. (2005) Evaluation of TIG flux welding on the characteristics of stainless steel. *Science and Technology of Welding and Joining*; 10, 566–573.



S. I. Bachani is an Assistant Professor in Mechanical Engineering Department, Dr. Jivraj Mehta Institute of Technology, Anand, Gujarat. His area of interest are Industrial Engineering, Manufacturing Engineering and Machine Design. He has published research articles in International Conference.



Dr. N D Ghetiya is an Associate Professor in the Mechanical Engineering, Institute of Technology, Nirma University, Ahmedabad. He has received his post graduate degree from IIT, Bombay with manufacturing Engineering as specialization and Ph. D in the area of friction stir welding. His research interest includes Material Science, Manufacturing Processes and their analysis.